




# Differential modulation of thermal preference after sensitization by optogenetic or pharmacological activation of heat-sensitive nociceptors

Molecular Pain  
Volume 17: 1–17  
© The Author(s) 2021  
DOI: 10.1177/17448069211000910  
journals.sagepub.com/home/mpx  


Jerry Li<sup>1</sup> , Maham Zain<sup>2</sup>, and Robert P Bonin<sup>2,3</sup> 

## Abstract

Common approaches to studying mechanisms of chronic pain and sensory changes in pre-clinical animal models involve measurement of acute, reflexive withdrawal responses evoked by noxious stimuli. These methods typically do not capture more subtle changes in sensory processing nor report on the consequent behavioral changes. In addition, data collection and analysis protocols are often labour-intensive and require direct investigator interactions, potentially introducing bias. In this study, we develop and characterize a low-cost, easily assembled behavioral assay that yields self-reported temperature preference from mice that is responsive to peripheral sensitization. This system uses a partially automated and freely available analysis pipeline to streamline the data collection process and enable objective analysis. We found that after intraplantar administration of the TrpVI agonist, capsaicin, mice preferred to stay in cooler temperatures than saline injected mice. We further observed that gabapentin, a non-opioid analgesic commonly prescribed to treat chronic pain, reversed this aversion to higher temperatures. In contrast, optogenetic activation of the central terminals of TrpVI<sup>+</sup> primary afferents via *in vivo* spinal light delivery did not induce a similar change in thermal preference, indicating a possible role for peripheral nociceptor activity in the modulation of temperature preference. We conclude that this easily produced and robust sensory assay provides an alternative approach to investigate the contribution of central and peripheral mechanisms of sensory processing that does not rely on reflexive responses evoked by noxious stimuli.

## Keywords

Behavioral analysis, thermal preference, optogenetics, TrpVI

Date Received: 24 January 2021; Revised 24 January 2021; accepted: 10 February 2021

## Introduction

Chronic pain is pain that persists for more than three months without clear protective benefits and can be a disease by itself or arise from another underlying health condition. These conditions may be precipitated by a series of events or a combination of various risk factors that affect multiple dimensions of an individual's daily life, including their emotional wellbeing, ability to perform daily tasks, and functioning in the workplace.<sup>1–3</sup> On a cellular level, pathological pain can arise from neurochemical and circuit level reorganization of primary afferents and spinal dorsal horn neurons.<sup>4,5</sup> These changes not only manifest in the form of hyperalgesia, where a painful stimulus is perceived as more painful, but also allodynia where innocuous stimuli can also

begin to evoke pain. Thermal and mechanical allodynia are features of many clinical pain conditions.<sup>6–8</sup> These are highly debilitating as they make innocuous stimuli

<sup>1</sup>Department of Human Biology: Neuroscience and Immunology, University of Toronto, Toronto, Ontario, Canada

<sup>2</sup>Leslie Dan Faculty of Pharmacy, University of Toronto, Toronto, Ontario, Canada

<sup>3</sup>University of Toronto Centre for the Study of Pain, University of Toronto, Toronto, Ontario, Canada

The first two authors contributed equally to this work.

### Corresponding Author:

Robert P Bonin, Leslie Dan Faculty of Pharmacy, University of Toronto, 144 College Street, Room 1004, Toronto, Ontario M5S 3M2, Canada.  
Email: rob.bonin@utoronto.ca



such as warm water, a light breeze, and the feeling of clothing against skin painful.

The mechanistic and behavioral examination of the changes in sensory processing that accompany pathological pain are critical to the understanding of chronic pain pathology and development of novel pain therapeutics.<sup>9</sup> For many years now, little translational success has placed current paradigms of pathological pain into question.<sup>9,10</sup> In preclinical studies of mice, researchers cannot directly assess pain perception in the animals and are limited to quantifying indirect behavioral or physiological measures of pain. The most widely used assays for studying pain use acute noxious stimuli to elicit reflexive, nocifensive behaviors, such as limb withdrawal, grooming, or paw licking. Typical stimulus-evoked pain assays include the Hargreaves test, von Frey filaments, and cold or hot plate tests.<sup>11,12</sup> However, these assays fail to capture ongoing sensory changes in pain and rely on exposure to noxious stimuli that are infrequently experienced by patients. These assays are also often labour-intensive and require extensive experimenter intervention, thus lending them to increased subjectivity.<sup>13</sup> Moreover, reflexive nocifensive responses can be purely spinal cord-mediated and can still be seen in anesthetized animals,<sup>11,14,15</sup> and may not accurately reflect chronic pain conditions that involve complex supraspinal sensory integration. These concerns have led to increased usage of unconditioned or non-evoked behavioral responses with the aim of capturing endogenous indicators of spontaneous or ongoing pain.<sup>11</sup> Such measures include operant assays, the Mouse Grimace Scale,<sup>16,17</sup> automated behavioral tracking,<sup>11</sup> weight-bearing or gait analysis, nesting or burrowing behavior, ultrasonic vocalizations, and free-choice temperature preference.<sup>18,19</sup> Along with increased adoption of assays for spontaneous pain, there has also been an increase in the automation of data collection. Automated analyses allow for reduced subjectivity by minimizing animal handling and removing the need for physical restraints, thereby reducing stress on the animals.

The automated assessment of thermal preference provides a non-invasive approach to study behavioral phenotypes emerging from central and peripheral mechanisms of sensitization. Changes in thermal sensitivity can arise following activation of nociceptors expressing the transient receptor potential cation channel subfamily V member 1 (TrpV1) protein that is activated by noxious heat (>43°C), endogenous lipids such as anandamide, plant derivatives such as capsaicin and acidity.<sup>20–23</sup> Thermal sensitization can consist of thermal hyperalgesia and/or allodynia, yet much of the existing literature focuses on thermal hyperalgesia as measured by changes in withdrawal thresholds to noxious temperatures.<sup>24–27</sup> Aversion or nocifensive responses to innocuous cold and warm temperatures, termed cold or heat allodynia, have

also been observed in pain models. The incidence of thermal allodynia is partially determined by type of pain model used, as heat allodynia has been more consistently shown in inflammatory pain models as opposed to neuropathic pain models,<sup>27–29</sup> while cold allodynia is often a prominent feature of neuropathic pain.<sup>30</sup> Capsaicin, a TrpV1 agonist, has been shown to produce significant thermal allodynia and hyperalgesia in both humans and animals via activation of TrpV1.<sup>20</sup> TrpV1 expression in the adult mouse sensory afferents is mostly restricted to peptidergic C-fibers, a primary afferent subtype that is known to be critical for the relay of nociception.<sup>31</sup> In addition, recent strides in the development of transgenic animals and optogenetics have allowed precise optical control of TrpV1-expressing afferents. Specifically, in mice expressing the light-activated excitatory ion channel channelrhodopsin (ChR2) in TrpV1<sup>+</sup> primary afferents, the delivery of blue light to the periphery induces nocifensive behaviors and withdrawal from the light stimulus.<sup>32,33</sup> The majority of optogenetic pain research has used transdermal light to activate the primary afferents; while this is a non-invasive strategy, it restricts the delivery of light to the periphery and can complicate experiments involving concurrent optogenetic and thermal or mechanical stimulation.<sup>32,34</sup> The development of novel surgical techniques enables non-restrictive optogenetic control of defined afferents and the study of how defined nociceptor populations contribute to nociceptive processing and pain-associated behavior.<sup>35–37</sup>

The complementary approaches of non-invasive behavioral testing and optogenetics allow for investigation into whether free choice temperature preference of mice can serve as a measure of changes in thermal sensitivity, and thermal allodynia in particular. Given the need for improved approaches to non-invasively study pathological sensory processing and associated behaviors, we created an automated assay for the assessment of thermal preference in mice and studied changes in thermal preference following pharmacological and optogenetic modulation of activity of the TrpV1 expressing nociceptors.

## Materials and methods

### *Thermal preference arena development and calibration*

A linear temperature gradient was created across a thin, 40.6 × 10.2 cm plate of aluminum metal (Figure 1(a) and (b)) and powered by rerouting different outputs from a 480 W ATX computer power supply to each electrical component. Three 40 mm × 40 mm 50 W Peltier thermoelectric devices (TEC1-1270640; Hubei I.T., Shanghai) were used to create the gradient. Two Peltier devices

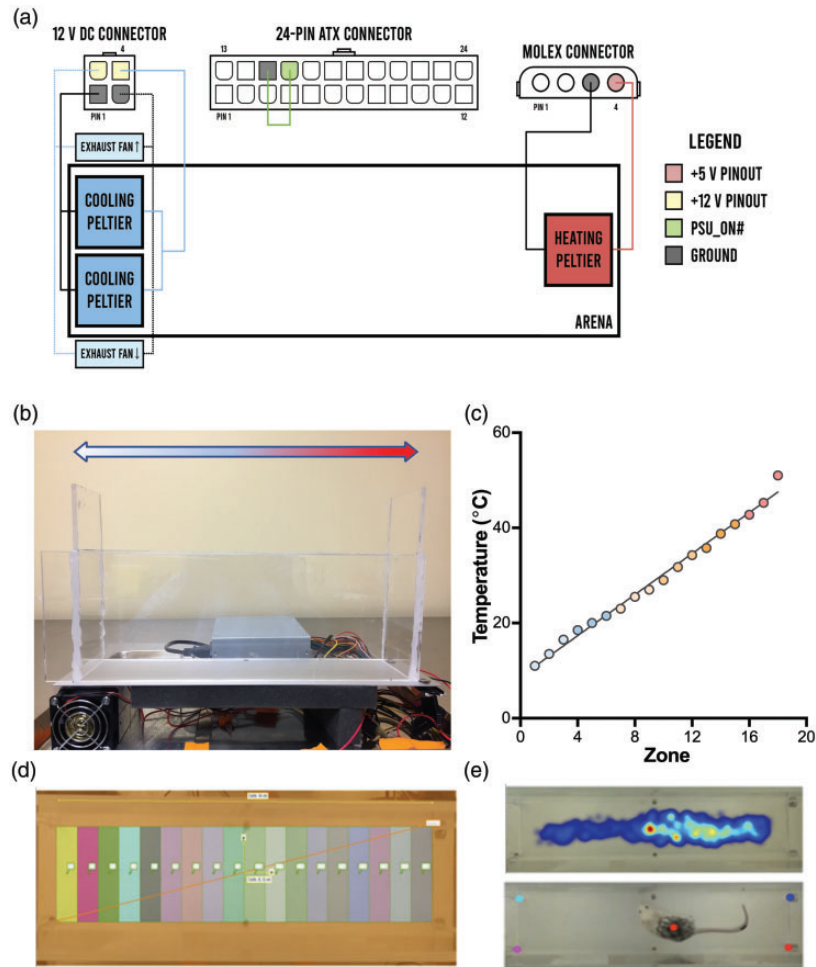


**Figure 1.** Automated assay setup and tracking parameters. (a) Circuit diagram indicating wiring, connections, and parts required to reproduce setup. Two cooling Peltier devices and fans were each wired to +12 V connections and ground pins from the 12 V DC connector, while a single warming device was wired to the +5 V pinout from the Molex connector. A short circuit was made between the green, 16th pin (PSU\_ON#) and adjacent ground pin to turn on the power supply. (b) A profile of the arena in which mice were placed, tracked with a camera directly above. Peltier devices, powered by a 480 W computer power supply, on either ends of an aluminum plate maintained a linear temperature gradient from  $11.0 \pm 0.6$  (blue) to  $51.0 \pm 0.7^\circ\text{C}$  (red). (c) Linear temperature gradient ( $r^2 = 0.89$ ), with each point, or zone, corresponding to measurements taken with an infrared thermometer every 2.0 cm of the arena. (d) Eighteen evenly spaced, arbitrarily coloured, 2.0 cm divisions across the arena that correspond to different temperature zones tracked by EthoVision. (e) *Top*: EthoVision's heatmap analysis of mouse movement throughout the arena in one trial. Mouse position was determined by the location of their centre, as shown in the bottom image. Warmer temperatures correspond to longer time spent in those regions. *Bottom*: DeepLabCut tracking the mouse's centre in the same trial. Four points on each corner of the arena were used to calculate the position of the mouse.

were mounted beside each other on the underside of one end of the aluminum sheet to provide cooling, while another was mounted on the opposite end in the opposite configuration to heat the aluminum sheet and create the gradient. The Peltier devices were attached to the aluminum sheet with thermoconductive paste to optimize heat transfer. The two cooling Peltier devices were each connected in parallel to a +12 V pin and a ground pin from the 12 V direct current (DC) connector, while the single heating device was connected to a +5 V pin and ground pin from the Molex connector. The Peltier devices providing cooling were each mounted

on  $6.5\text{ cm} \times 6.5\text{ cm} \times 6.5\text{ cm}$  aluminum heat sinks. Heat was dissipated from the heat sinks via two 6 cm cooling fans, with their exhaust direction pointed away from the heat sinks. The fans were connected in parallel to the remaining +12 V pin and ground pin from the 12 V DC connector. Lastly, a jumper wire was placed between the green, 16th pin (PSU\_ON#) and an adjacent ground pin on the 24-pin ATX connector to allow the power supply to turn on (Figure 1(a)). The level of noise produced by the power supply and fans cooling the Peltier devices was measured for 5 minutes at stable temperatures using the iOS app, Decibel X, version 7.0.0.

The cold, middle, and hot ends of the assay averaged noise levels of 70.5, 68.3, and 67.9 dB, respectively. Four walls of plexiglass lined with black paper on the outer sides were then used to create a  $36.0 \times 7.4$  cm arena atop the aluminum in which mice could freely explore. Lastly, a Sony HDR-CX405 video camera was set up directly above the arena to record 30-minute trials. Before each trial, the arena's temperature gradient was calibrated by turning on the Peltier devices for 15 to 20 minutes and temperature measurements were taken with an infrared thermometer at several points along the aluminum sheet.

### Animals and housing

All experiments were conducted in accordance with the Canadian Council on Animal Care and the University of Toronto's Animal Care and Use guidelines. Adult (>8 weeks old), male CD-1 mice were used for the capsaicin-induced sensitization experiments. 7-week old male CD-1 mice were supplied by Charles River Laboratories and housed in identical enriched home cages in groups of 3–4 upon arrival. They were given a week to habituate to the housing facility, with a  $23.0 \pm 0.5^\circ\text{C}$  ambient temperature,  $53 \pm 13\%$  relative humidity, and 14 h light:10 h dark cycle. Experiments were conducted on mice 8–16 weeks of age during the light cycle. Food and water were given *ad libitum* in their home cages throughout experiments. CD-1 mice were marked on their tails and backs for identification and video tracking, respectively, using a black permanent marker 24 hours before trials began, and any re-marking, if necessary, at least 30 minutes before each trial. Mice were placed in the powered-on and fully calibrated arena to habituate to the assay for 30 minutes before each trial.

Adult male (>12 weeks old) TrpV1-ChR2 male mice were used for the optogenetic sensitization experiments and adult male (>12 weeks old) C57BL/6N male mice were bred in-house and used to study the effects of the surgical strategy on mouse well-being. All mice were kept in groups of 1 to 4 mice per cage prior to ferrule implantation and singly housed after the implantation surgery with food and water provided *ad libitum*. Mice expressing ChR2 in TrpV1<sup>+</sup> nociceptive afferents (TrpV1-ChR2) were generated by crossing mice expressing Cre-recombinase in TrpV1<sup>+</sup> neurons with mice expressing a loxP-flanked STOP cassette upstream of a ChR2-EYFP fusion gene at the Rosa 26 locus (Rosa-CAG-LSL-ChR2(H134R)-EYFP-WPRE; stock number 012569, The Jackson Laboratory, Bar Harbor, ME).

### Capsaicin and gabapentin treatments

Two separate randomized crossover studies were conducted. For the first set of trials, 30 minutes after an

ipsilateral hind paw injection of either saline (5  $\mu\text{L}$ ) or capsaicin (5  $\mu\text{L}$ , 0.5% w/v dissolved in 1:1:8 95% ethanol:Tween 20:saline), each mouse was recorded in the arena for 30 minutes (Figure 2(a)). For the second set of trials, each mouse first had an intraperitoneal injection of either saline (control) or gabapentin (100 mg/kg), and then after 30 minutes, an ipsilateral hind paw injection of capsaicin of the same concentration (Figure 2(b)). Previous work done in our lab has shown that gabapentin at 100 mg/kg produces analgesia without impacting locomotion in mice.<sup>38</sup> After another 30 minutes, they were recorded in the arena for 30 minutes. All capsaicin injections were conducted after placing the mice under light isoflurane anesthesia, with toe-pinch reflex present. By the end of each set of trials, each mouse served as their own control and had injections of both control and treatment, with a 48-hour washout between each treatment. For each mouse, after the initial control or treatment injection, subsequent trial injections were done in the contralateral hind paw. All capsaicin and gabapentin injections were done using a 50  $\mu\text{L}$  Hamilton syringe and 1 mL syringe, respectively, fitted with 30-gauge needles. All drug administrations were performed by a blinded experimenter.

### Ferrule production and implantation for optogenetic light delivery

The surgical approach for the optogenetic experiments was adapted from the protocols for *in vivo* optogenetics described recently.<sup>35,37</sup> The prepared ferrule was sterilized with 70% ethanol and consisted of a 1.25 mm fiber optic ferrule (Ceramic ferrule, 1.25 mm diameter, 440  $\mu\text{m}$  bore; Thor Labs, Germany) with a 400  $\mu\text{m}$  fiber optic core (Multimode fiber, 400  $\mu\text{m}$  core, 0.39 NA; Thor Labs, Germany) that protruded out at a maximum length of 0.5 mm from the concave side of the ferrule. Mice were initially anesthetized using 5% isoflurane and then maintained on 2–2.5% isoflurane in a stereotaxic frame. The back of the mouse was shaved and a 1.5 cm incision was made centered around the peak of the dorsal spinal curvature. Small spring scissors were used to make shallow incisions lateral to the T13 vertebrae which was identified based on its location relative to the peak of the dorsal spinal curve and the lowest rib. The vertebra was clamped using 2 pairs of transverse spinal adapters (Stoelting Co., Wood Dale, IL, USA) and the flesh was removed using spring scissors and fine forceps. Bleeding was controlled using autoclaved Kimwipes and absorbable gelatin sponges (Gelfoam; Pfizer Inc., New York, NY, USA). After ensuring stability of the vertebrae, a microdrill was used to flatten down the spinous process and slightly abrade the surface of the bone to promote adhesive bonding. The microdrill was then used to drill a hole in the center of the right side of the

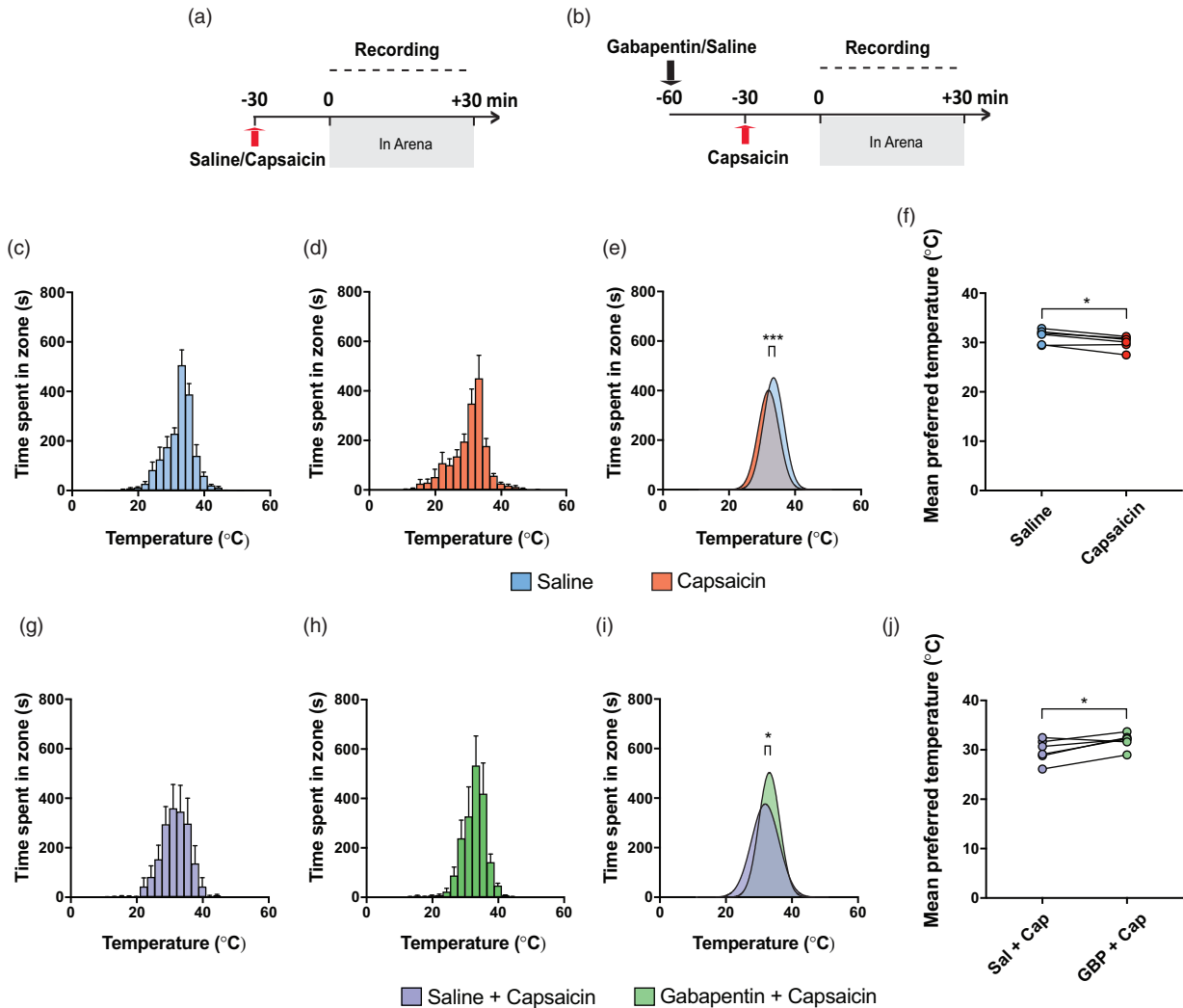


**Figure 2.** Gabapentin prevented capsaicin-induced change in thermal preference. (a) Experimental timeline for capsaicin or saline injection. (b) Experimental timeline for trials with gabapentin or saline injection before the capsaicin injection. Total time spent in each temperature zone after saline (c), capsaicin (d), saline + capsaicin (g), or gabapentin + capsaicin (h) administration, measured by EthoVision. Error bars represent SEM. Comparison of mean preferred temperature between treatment groups showed capsaicin-treated mice preferred a cooler temperature of  $31.3 \pm 0.3^\circ\text{C}$ , than did saline-treated mice, that preferred  $32.7 \pm 0.3^\circ\text{C}$  (e). Conversely, gabapentin administration before capsaicin prevented heat aversion from occurring (i), as demonstrated by gabapentin-treated mice that preferred a warmer temperature of  $32.4 \pm 0.3^\circ\text{C}$  versus saline-treated ones, that preferred  $31.2 \pm 0.4^\circ\text{C}$ . (f and j) Paired *t*-tests of individual mice's mean preferred temperatures further reflected avoidance of higher temperatures in mice that received capsaicin (f), whereas this was prevented in mice that received gabapentin (j). Sal, saline; Cap, capsaicin; GBP, gabapentin. \* $p < 0.05$ , \*\*\* $p < 0.001$

vertebra. Once spinal tissue was visible through the burr hole, the surgical site was cleared of any bone fragments and the prepared ferrule was lowered in place using stereotactic arms and cemented in place using Superglue and C&B Metabond (Parkell Inc., Brentwood, NY, USA). The skin around the implant was closed using a surgical adhesive (GLUture; Zoetis Inc., Parsippany-Troy Hills, NJ, USA). In the sham surgery animals, all surgical manipulation was performed except for the placement of the implant and its accompanying adhesives. The mice were allowed to recover for a minimum of 2 weeks prior to any behavioral testing.

### Optogenetic light delivery

The implant in the mouse was coupled to a patch cable (400  $\mu\text{m}$  core, 0.39 NA; Thor Labs, Germany) using a mating sleeve. The intensity and frequency of the 470 nm laser was controlled using a LED driver (Thor Labs) and a pulse width modulator (XY-LPWM; Protosupplies, USA), respectively. The laser output intensities reported here refer to the light intensity output from a test implant coupled to a patch cable through a mating sleeve. The output light intensity, measured using a PM100 light meter (Thor Labs), was calibrated

with the current input from the LED driver. To determine the threshold light intensity for behavioral response, the patch cable was coupled to the implant while the mouse was under light isoflurane anesthesia. Each mouse was given 20 minutes to recover from the anesthetic and habituate to the fiber. The light intensity was increased in incremental steps of 0.2 mW with each intensity being presented at a maximum of 20 seconds or until a nocifensive response was observed. The first intensity level at which nocifensive responses like biting of the hind leg, fleeing and vocalization were first observed was classified as the threshold light intensity. Changes in thermal preference were assessed during acute peri-threshold stimulation and post suprathreshold stimulation of the TrpV1<sup>+</sup> neurons. Acute peri-threshold stimulation was performed 2 weeks post-operation and consisted of photo-activation at a frequency of 10 Hz with intensity being set at 80% of the threshold light intensity. Suprathreshold stimulation was performed in the same mice 1 week after peri-threshold stimulation at 2 Hz at 200% of the threshold light intensity. 2 Hz light stimulation has been shown to produce optogenetically-induced LTP in *ex vivo* spinal cord slices.<sup>39</sup>

### Behavioral assessment of implanted mice

These experiments were performed 2 weeks post-operation in 15-week old male ferrule implanted and non-implanted sham surgery C57BL/6N mice

### Rotarod

Evoked motor activity was tested in ferrule implanted and non-implanted sham surgery C57BL/6N mice using a rotarod (Bioseb, Chaville, France). Rotation was started immediately after the mice were placed on the rotarod, and accelerated from 4 to 40 RPM over a period of 120 s. The latency to fall was measured and a cut-off time of 120 s was set. Trials were repeated five times per mouse separated by 30 min each.

### Open field

Spontaneous locomotion and anxiety related behaviors were assessed in ferrule implanted and non-implanted sham surgery C57BL/6N mice using an open field assay. The open field assay was conducted in a dimly illuminated square box. The floor of the box measured 30 × 30 cm. The mice were allowed to explore the novel box for 15 minutes while they were video recorded using an overhead video camera. The videos were later analyzed using EthoVision XT (Noldus Inc., Wageningen, Netherlands). The center point of the mouse was tracked, and total distance travelled, and time spent in the center zone of the assay was analyzed.

### Mechanical sensitivity

Mechanosensitivity was assessed using von Frey filaments. Mice were placed in a small chamber with a grid floor and allowed to habituate for 30 minutes. Both hind paws were tested using the SUDO method<sup>40</sup> and the paw withdrawal threshold was reported in pressure (g/mm<sup>2</sup>).<sup>41</sup> This distinction in paw was relevant since the implant was always fixed on the right side of the vertebrae and we therefore expected possible lateralization in terms of behavioral or sensory deficit produced as the result of the implant.

### Analysis of thermal preference

EthoVision was used to calculate the cumulative amount of time each mouse spent in different temperatures across the arena. The 36.0 cm length of the arena was separated into eighteen 2.0 cm temperature zones (Figure 1(d)). Heatmaps were generated along with coordinates of each mouse's centre-point position, hereafter referred to as centre, within the arena (Figure 1(e)). Coordinate samples were taken once per second for each 30-minute trial, for a total of 1800 coordinates per trial. Raw coordinates were given in centimetres and converted into pixels for comparison with DeepLabCut's raw coordinates.

DeepLabCut (version 2.0.4.1, <http://www.mousemotelab.org/deeplabcut>) was used to validate EthoVision's tracking data (Figure 1(e)). DeepLabCut is an open-source animal tracking program that uses deep neural networks to recognize labelled points in videos.<sup>16</sup> DeepLabCut's tracking algorithm was trained to recognize the mouse's centre, labelled as visually close to EthoVision's calculated centre as possible, with 200 distinct marked reference frames. All other settings were left as default as specified in the setup protocol.<sup>42,43</sup> No further refinement of tracked points were performed after training. All training and video analyses were done using an NVIDIA GeForce RTX 2080Ti supported by an Intel® Core™ i7-4790 and 16 GB of RAM, on Ubuntu 18.04.2. Similarly, 1 coordinate sample was taken per second for each 30-minute trial by averaging the positions for all 30 frames each second, for a total of 1800 coordinates per trial. Raw coordinates were obtained in pixels and converted into centimetres and zones for further validation of EthoVision's raw coordinates. All trial recordings were recorded at 30 frames per second and normalized to a 16:9 aspect ratio, 1280x720 resolution using a scaling factor for data analysis.

Video recordings obtained for the assessment of thermal preference in the optogenetic experiments were also manually scored for nocifensive behaviors using a macro

in Microsoft Excel. All EthoVision analysis and manual video scoring were done in a blinded manner.

### Statistical analysis

Mean temperature preferences were determined by fitting data to a Gaussian distribution with least squares regression and no special handling of outliers. These means of the controls and treatments were then compared through a parametric paired two-tailed *t*-test. Any unpaired mice were excluded from the calculation of statistical significance. The performance of implanted and sham surgery animals in behavioral experiments was compared using unpaired two-tailed *t*-tests and repeated measures two-way analysis of variance (ANOVA). Paired two-tailed *t*-tests and repeated measures one-way ANOVA were used to compare means in the behavioral experiments conducted to validate our optogenetic stimulation protocols. All statistical analyses were performed in GraphPad Prism 8, with a significance level set at  $P < 0.05$ . Data are presented as mean  $\pm$  standard error of the mean (SEM).

## Results

### Arena calibration

To confirm the arena had a linear temperature gradient, the temperature of the arena floor was measured every 2.0 cm along its length with an infrared thermometer every 5 minutes for 1 hour. Once temperatures of the floor stabilized, the cold, middle, and hot ends measured temperatures of  $11.0 \pm 0.6^\circ\text{C}$ ,  $29.0 \pm 0.9^\circ\text{C}$ , and  $51.0 \pm 0.7^\circ\text{C}$ , respectively, and a clear linear gradient was observed along the length of the arena (Figure 1(c)).

### Capsaicin shifted temperature preference towards lower temperatures

We first used the thermal preference assay to examine whether intraplantar capsaicin would produce a change in mouse thermal preference. We first performed an intraplantar injection of either saline or capsaicin into the mouse hind paw 30 minutes prior to testing in a randomized crossover manner (Figure 2(a)). We found that mice injected with saline showed a preference for a temperature of  $32.7 \pm 0.3^\circ\text{C}$  (Figure 2(c)), whereas those treated with capsaicin preferred a slightly cooler temperature of  $31.3 \pm 0.3^\circ\text{C}$  (Figure 2(d)). Comparing both groups via Gaussian fit of each treatment group's summed positional data over the experiment revealed a small but significant difference between preferred temperatures across the two treatment groups, with capsaicin-treated mice preferring cooler temperatures (Figure 2(e);  $F_{(3, 264)} = 8.53$ ,  $p < 0.0001$ ). Moreover, this

shift to cooler temperatures was seen within mice with paired analysis of mean preferred temperature after each treatment, indicating that mice consistently showed a preference for cooler temperatures after capsaicin was administered (Figure 2(f); Paired *t*-test,  $t_5 = 3.52$ ,  $p = 0.017$ ).

### Gabapentin prevented capsaicin-induced heat aversion

To assess if the capsaicin-induced avoidance of higher temperatures was a result of pain associated with capsaicin injection rather than a systemic change in thermal preference, we administered either saline or a non-opioid analgesic, gabapentin, 30 minutes prior to capsaicin injection (Figure 2(b)). Mice that received saline and capsaicin preferred  $31.2 \pm 0.4^\circ\text{C}$  (Figure 2(g)), whereas mice that received gabapentin and capsaicin preferred  $32.4 \pm 0.3^\circ\text{C}$  (Figure 2(h)). Comparing these two groups with a Gaussian fit of the summed treatment group positional data similarly revealed a small but significant difference between their mean preferred temperatures, with gabapentin and capsaicin treated mice preferring higher temperatures compared to mice that were only treated with capsaicin (Figure 2(i);  $F_{(3, 264)} = 3.74$ ,  $p = 0.012$ ). As before, this difference in temperature preference was observed within mice as a paired analysis consistently revealed a preference for higher temperatures after treatment with gabapentin (Figure 2(j); Paired *t*-test,  $t_5 = 3.06$ ,  $p = 0.028$ ).

### DeepLabCut provides an open-source approach to the assessment of mouse thermal preference

The positional analysis completed thus far employed EthoVision, which is a versatile and commonly used commercial behavioral tracking and analysis program. EthoVision tracks animals via the contrast between the animal and the background to assess the frame-by-frame position of the animals and/or several body parts to calculate a range of parameters including locomotion, velocity, and activity.<sup>44–46</sup> We further assessed whether an open-source tracking software, DeepLabCut, could similarly be used to detect positional differences described in the thermal preference assays above as a free alternative to EthoVision.

We first confirmed that DeepLabCut could track the position of the centre of the mouse similarly to EthoVision. The DeepLabCut training labels were created as visually close to EthoVision's centre as possible before training its tracking algorithm. After training the network with  $>1,000,000$  iterations, the network was able to detect the center of the mouse with an accuracy of  $\pm 4.32$  pixels (equivalent to  $\pm 0.17$  cm) in test videos compared to EthoVision. The mean temperature

preference for each mouse tested above was then determined by EthoVision and DeepLabCut. Across all mice there was an extremely high correlation between the mean preference assessed with the two methods (Figure 3(a); Pearson's  $r=0.94$ ), indicating that DeepLabCut can be used to assess mouse thermal preference. Moreover, we detected no significant differences in the mean temperature preference of any treatment group when comparing between analysis approaches (Figure 3(b) and (c)).

To compare approaches at a pixel-level of tracking in all samples, we then calculated the distance between EthoVision and DeepLabCut's predicted centre location for every frame in the first trial of each treatment group (Figure 3(c)). We found that the 95% confidence interval of the median difference was -0.048 cm to 0.021 cm, with a minimum and maximum difference in centre points of

-2.67 and 2.62 cm, respectively. Negative values represent samples where DeepLabCut's predictions visually fell to the left of the mouse, while positive values are to the right. Because even the most extreme differences did not exceed the visual size of the mice, these data indicate that DeepLabCut largely provided the same frame-by-frame precision observed with EthoVision.

Finally, we repeated the positional analysis of mice treated with saline or capsaicin, and capsaicin or capsaicin + gabapentin (Figure 2). As seen with EthoVision, our positional analysis with DeepLabCut revealed that mice treated with capsaicin preferred cooler temperatures than mice treated with saline (Figure 3(d) to (g)), and that mice treated with gabapentin and capsaicin preferred warmer temperatures than those treated with saline and capsaicin (Figure 3(h) to (k)). With similar findings to EthoVision, mice treated with saline and

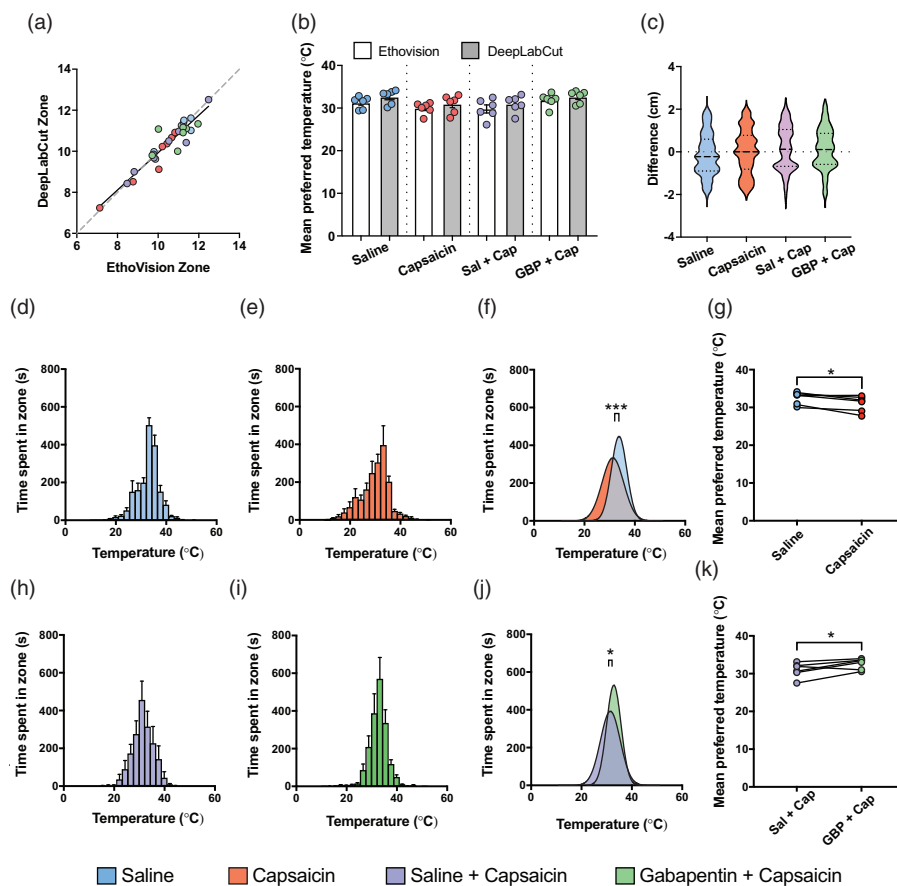


**Figure 3.** DeepLabCut and EthoVision provided equal animal tracking precision in the thermal preference assay. (a) Comparison of each mouse's mean preferred temperatures ( $n=31$ ) determined by DeepLabCut and EthoVision showed that DeepLabCut could track mice's centres with high precision, comparable to that of EthoVision (Pearson's  $r=0.94$ ). (b and c) There was no difference in mean preferred temperature obtained for each of the groups by both software using a one-way ANOVA. ( $n=6$ ) Total time spent in each temperature zone after saline (d), capsaicin (e), saline + capsaicin (h), and gabapentin + capsaicin (i) administration, measured by DeepLabCut. Error bars represent SEM. Comparing mean preferred temperatures measured by DeepLabCut validated that capsaicin indeed shifted temperature preference to cooler temperatures (f) and that gabapentin prevented this from occurring (j). Paired  $t$ -tests of individual mean preferred temperatures reflected a shift in preference to cooler temperatures post-capsaicin administration (g) that was no longer seen if gabapentin was given before capsaicin (k). Sal, saline; Cap, capsaicin; GBP, gabapentin; ANOVA, analysis of variance. \* $p < 0.05$ , \*\*\* $p < 0.001$



capsaicin preferred temperatures of  $33.7 \pm 0.2^\circ\text{C}$  and  $31.2 \pm 0.3^\circ\text{C}$ , while those treated with saline or gabapentin before capsaicin preferred  $31.5 \pm 0.3^\circ\text{C}$  and  $32.9 \pm 0.2^\circ\text{C}$ , respectively. These data further support that DeepLabCut provides an open-source option for the analysis of mouse thermal preference as assessed using the low-cost thermal preference assay described here.

### Optogenetic activation of the central terminals of *TrpVI*<sup>+</sup> afferents did not recapitulate changes in thermal preference induced by intraplantar capsaicin

Having established that capsaicin can produce an aversion to warmer temperatures we sought to assess whether optogenetic activation of the central terminals of the *TrpVI*<sup>+</sup> afferents would similarly shift thermal preference. To deliver light to our region of interest the ferrule implant was fixed in the T13 vertebra that overlies a portion of the L4-L6 spinal cord region that receives innervation from the hindlegs of the mouse (Figure 4 (a)). The implant was well tolerated by mice, with most animals retaining implants for a minimum of 2 months. To ensure that the implant had limited impact on mouse motor and sensory function, we assessed evoked motor

activity, spontaneous locomotion and mechanical sensitivity using rotarod, open field and von Frey filaments, respectively, in ferrule implanted and sham operated C57BL/6N mice. There was no difference in performance on the rotarod between sham and implanted animals (Figure 4(b); Repeated measures two-way ANOVA, effect of treatment:  $F_{(1, 4)} = 0.15$ ,  $p = 0.72$ , effect of trial:  $F_{(1.8, 7.2)} = 4.08$ ,  $p = 0.070$ , effect of interaction:  $F_{(4, 16)} = 0.52$ ,  $p = 0.73$ ). There was also no difference in distance travelled in the open field assay (Figure 4(c); Unpaired *t*-test,  $p = 0.32$ ). Overall, these data indicate there was no difference in both evoked and spontaneous motor activity between the two experimental groups. Additionally, time spent in the center zone was analyzed in the open field to assess for thigmotaxis, an anxiety related behavior that can confound results of a preference-based assay like the one described within this paper. No differences were found for time spent in the center zone of the open field between implanted and sham mice (Figure 4(d); Unpaired *t*-test,  $p = 0.62$ ). Finally, no differences were found in the paw withdrawal thresholds of the ipsilateral and contralateral paws between the surgery and the sham animals, indicating that the implant did not change nociceptive

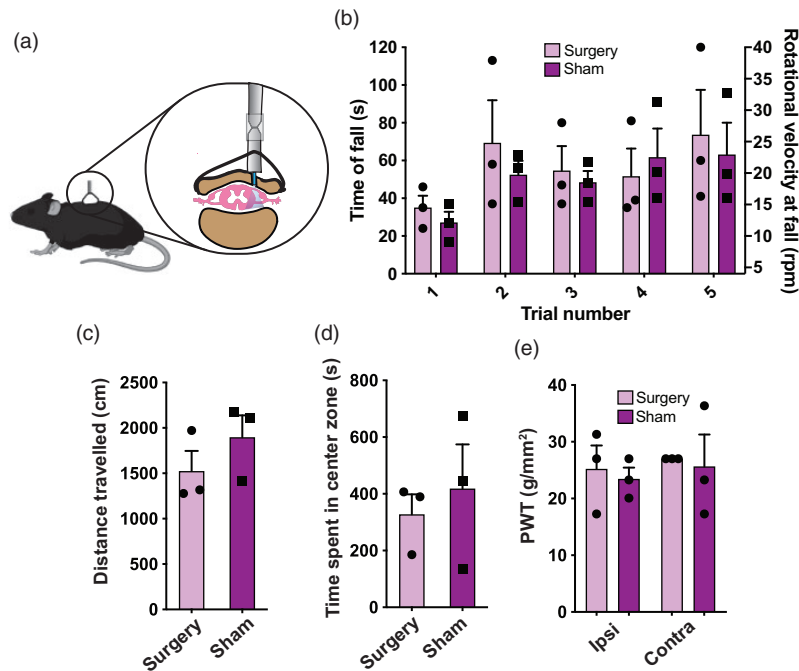


**Figure 4.** The ferrule implant surgery did not impact mouse sensory or motor behavior. (a) A cartoon illustration of the surgical strategy employed which depicts the placement of the implant relative to the vertebrae and spinal cord. (b) Evoked motor performance did not differ between implant surgery and sham surgery animals and was compared using a repeated measures two-way ANOVA. (c) No difference in distance travelled by implant surgery and sham surgery animals in open field assay as compared using an unpaired *t*-test. (d) No difference in time spent in center zone by implant surgery and sham surgery animals in open field assay as compared using an unpaired *t*-test. (e) Based on a repeated measures two-way ANOVA PWT of the ipsilateral and contralateral paws of the implant surgery and sham surgery animals did not differ.  $n = 3$  per group. Error bars represent SEM. ANOVA, analysis of variance; PWT, paw withdrawal threshold.

thresholds or cause sensory deficit (Figure 4(e); Repeated measures two-way ANOVA, effect of treatment:  $F_{(1, 4)}=0.17$ ,  $p=0.71$ , effect of paw:  $F_{(1, 4)}=0.34$ ,  $p=0.59$ , effect of interaction:  $F_{(1, 4)}=0.003$ ,  $p=0.96$ ). We used implanted TrpV1-ChR2 mice for the following experiments.

To assess whether stimulation of TrpV1<sup>+</sup> fibers is sufficient to induce changes in thermal preference, mice were connected to the LED light source and placed on the preference assay. Two different stimulation paradigms were used: (1) to assess whether peri-threshold stimulation can produce acute changes in thermal preference, mice were initially placed on the assay for 15 minutes with the LED off to establish baseline preference, after which peri-threshold stimulation (10 Hz, 80% threshold intensity) was then initiated for another 15 minutes (Figure 5(a)); (2) to assess whether stimulation at suprathreshold light intensities to initiate central sensitization would change temperature preference. In this paradigm, mice were placed on the assay for 15 minutes, after which they were removed from the assay and placed in an altered context where they received suprathreshold stimulation (2 Hz, 200% threshold intensity) for 10 minutes followed by a 30-minute wait time within that same context in accordance with previous studies of optogenetic sensitization.<sup>36,39</sup> The mice were then placed back on the assay for 15 minutes for assessment of temperature preference (Figure 5(b)).

The video recordings of the mice on the assay for the peri-threshold thermal assay experiments were manually scored for nocifensive licking and biting behavior. We found that mice spent more time engaging in licking and biting behavior during peri-threshold stimulation compared to the same mice prior to stimulation (Figure 5(c); Paired *t*-test,  $p=0.02$ ). Notably, the increased nocifensive behavior only emerged after the five minutes of peri-threshold stimulation (Figure 5(d); Repeated measures one-way ANOVA,  $F_{(2.6, 13.1)}=7.29$ ,  $p=0.01$ ). For the TrpV1-ChR2 mice stimulated with peri-threshold stimulation, mice had a thermal preference of  $38.3 \pm 0.7^\circ\text{C}$  at baseline (Figure 5(f)) prior to stimulation and a preference of  $38.6 \pm 0.6^\circ\text{C}$  during peri-threshold optogenetic stimulation of TrpV1<sup>+</sup> afferents (Figure 5(g)). Comparing the summed positional data of the animals at baseline and during peri-threshold stimulation revealed no difference in the Gaussian curves fit of the data sets (Figure 5(h);  $F_{(1, 210)}=0.10$ ,  $p=0.75$ ). Similarly, no within-mouse change in thermal preference was observed before and during peri-threshold stimulation (Figure 5(i);  $t_5=0.21$ ,  $p=0.84$ ), indicating that acute excitation of TrpV1<sup>+</sup> afferents does not modify thermal preference.

In order to confirm suprathreshold stimulation induced sensitization, we assessed mechanical paw withdrawal thresholds using von Frey filaments in TrpV1-

ChR2 and C57BL/6N mice that received suprathreshold stimulation. The suprathreshold stimulation intensity used for C57BL/6N mice was the average suprathreshold intensity from all TrpV1-ChR2 mice. Suprathreshold stimulation caused a decrease in the paw withdrawal threshold of the ipsilateral paw of the TrpV1-ChR2 mice but not the C57BL/6N mice (Figure 5(e); Repeated measures one-way ANOVA,  $F_{(1, 9, 9, 8)}=6.88$ ,  $p=0.01$ ) indicating that the change in mechanical sensitivity was not a non-specific effect of blue light. Having established that suprathreshold stimulation successfully induced mechanical hypersensitivity, we sought to assess whether it also induced changes in thermal preference. Overall, TrpV1-ChR2 mice exhibited a mean thermal preference of  $31.2 \pm 0.5^\circ\text{C}$  at baseline (Figure 5(j)) and  $33.5 \pm 0.3^\circ\text{C}$  after suprathreshold stimulation (Figure 5(k)). Comparing the summed positional data of the animals at baseline and after suprathreshold stimulation revealed that sensitization by optogenetic activation of central terminals of TrpV1<sup>+</sup> afferents unexpectedly produced a change in the overall positional distribution of animals towards warmer temperatures (Figure 5(l);  $F_{(1, 174)}=12.49$ ,  $p < 0.001$ ). This was in contrast to the opposite trend observed as a part of the capsaicin experiments. However, a paired *t*-test of the individual mouse temperature preferences failed to hold the same trend as the cumulative Gaussian fits (Figure 5(m);  $t_4=1.12$ ,  $p=0.33$ ).

## Discussion

Our findings show that an automated thermal selection assay can reveal subtle changes in thermosensory phenotypes in mice. We detected small, yet robust, differences in temperature preference pre- and post-capsaicin treatment using our minimally invasive assay using two different video assessment approaches. Our results also show that the changes in thermal sensitivity differ between mice injected with capsaicin, a TrpV1 agonist, versus those that have TrpV1<sup>+</sup> neurons activated optogenetically. Overall, the simplicity of our assay and ease of access to the materials and technologies used support its use as an easily implemented assay for investigation of new analgesic drugs.

The significant translational gap in pain research has promoted increased characterization of non-reflexive indicators of pathological sensory processing, as these may be of greater translational relevance.<sup>47</sup> As opposed to noxious stimulus-evoked pain assays, the investigation of behavioral responses of freely moving animals in response to environmental stimuli allows us to capture more subtle sensory and behavioral changes associated with pain states. Unlike nocifensive reflexes that can be evoked via spinal cord or subcortical circuits,<sup>11,14,15</sup> chronic pain involves a distributed nociceptive network

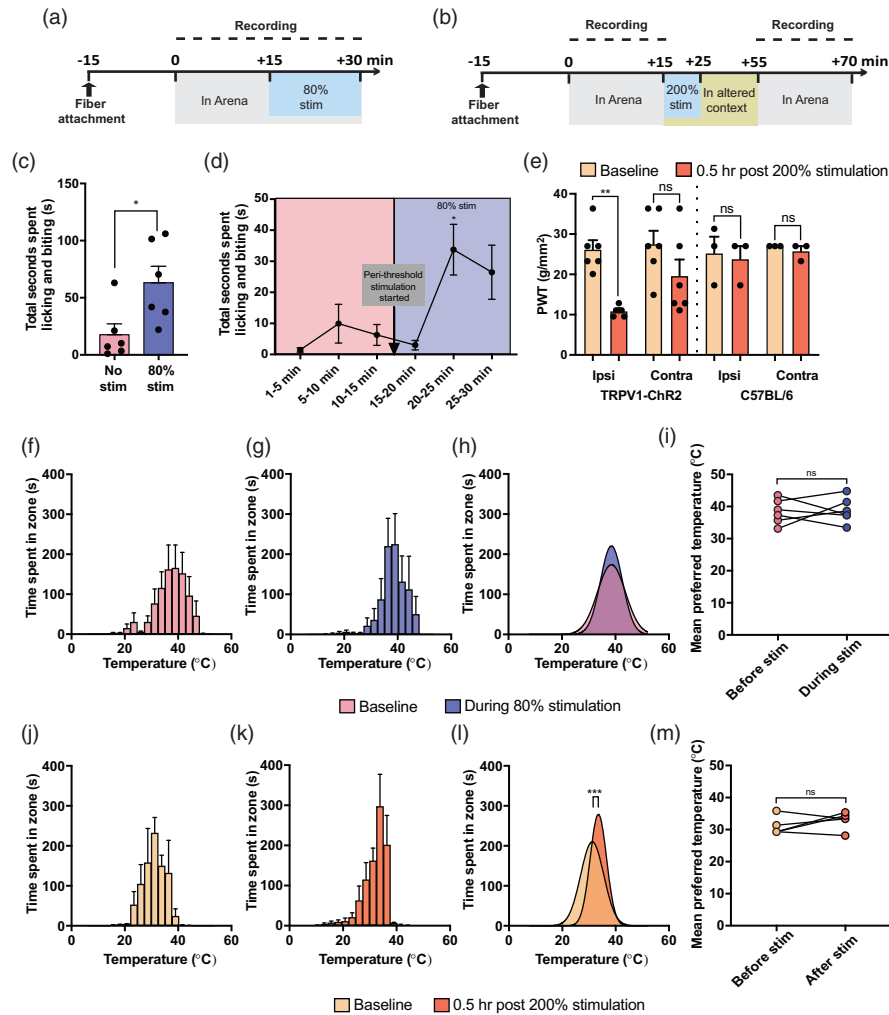


**Figure 5.** Optogenetic activation of the central terminals of the  $\text{TrpV1}^+$  afferents did not produce a shift in temperature preference. (a) Experimental timeline for assessing temperature preference before and during peri-threshold activation of  $\text{TrpV1}^+$  neurons. (b) Experimental timeline for assessing temperature before and after suprathreshold activation of  $\text{TrpV1}^+$  neurons. (c) Mice spent more time licking and biting their hindquarter during peri-threshold stimulation than under baseline and (d) these nocifensive behaviors emerged after more than 5 minutes of the peri-threshold stimulation being active ( $n = 6$ ). (e) Suprathreshold stimulation caused a decrease in the paw withdrawal threshold of the ipsilateral paw in only the  $\text{TrpV1-ChR2}$  mice ( $n = 3-6$  per group). Cumulative time spent in each temperature zone during (f) Pre-stimulation and (g) during stimulation for the peri-threshold stimulation experiments calculated using Ethovision. Cumulative time spent in each temperature zone during (j) Pre-stimulation and (k) after stimulation for the suprathreshold stimulation experiments calculated using Ethovision. (h) Comparison of the peaks of the Gaussian regressions fit to the aggregated data from all mice during pre-stimulation and stimulation conditions failed to reveal a shift in temperature preference during peri-threshold stimulation. (i) A paired t-test of temperature preferences of the individual mice, obtained through Gaussian fits to individual mouse data, also did not show a difference in preference under peri-threshold stimulation ( $n = 6$ ). (l) Comparison of the peaks of the Gaussian regressions fit to the aggregated data from all mice during pre-stimulation and post-stimulation conditions revealed that mice on average preferred a warmer temperature post-suprathreshold stimulation. (m) However, a paired t-test of mouse-specific temperature preferences did not uphold this trend and no differences were found in temperature preference pre- and post-suprathreshold stimulation ( $n = 5$ ). \* $p < 0.05$ , \*\* $p < 0.005$ , \*\*\* $p < 0.001$ ; ns, not significant.

that integrates supraspinal regions that control affective, cognitive, memory, and motor functions along with spinal cord nociceptive processing.<sup>48</sup> Therefore, a comprehensive preclinical assessment of pain would include measures for both acute and spontaneous behavioral responses to noxious and innocuous stimuli. Recent studies have characterized a variety of spontaneous

mouse behaviors that may be reflective of pain state, including free-choice temperature preference assays.<sup>10,11,13,16-19,38</sup> However, most assays used to assess thermal preference rely on mouse avoidance responses to noxious temperatures rather than assessment of native preference.<sup>11</sup> In contrast, our assay does not necessarily expose mice to noxious temperature

ranges and therefore provides a measure of response to innocuous temperature, allowing for a study of thermal allodynia or thermotaxis.

The selection of a preferred temperature by mice likely involves a complex evaluative process that integrates body temperature, environmental temperature, and the modulation of temperature sensation by pathological conditions, such as peripheral or central sensitization.<sup>49,50</sup> Thus, in direct contrast to reflexive responses in acute nociception assays, the preference of a particular temperature is driven by persistent sensory processing and the motivation to move to different temperatures may reflect non-reflexive and integrative sensory processing or coping behavior with important motivational or homeostatic components, such as avoiding pain or discomfort.<sup>51,52</sup> Additionally, given that mice are a prey species that tend to hide overt behavioral signs of pain or distress,<sup>12,15</sup> assays that rely on more subtle behavioral outputs, such as thermal selection, may provide a unique insight into subtle but physiologically relevant changes in sensory preferences and thresholds.

The intraplantar injection of capsaicin is associated with thermal and mechanical sensitization.<sup>24–26</sup> Our findings that intraplantar capsaicin injection induces a preference for cooler temperatures are consistent with these findings, as thermal sensitization and heat allodynia would be expected to produce an aversion to warm temperatures. Activation of TrpV1 receptors is not necessary for the expression of thermal preference as previous research has shown that TrpV1 knockout mice display normal behavior in thermal gradient assays.<sup>50,53</sup> This is not unexpected as TrpV1 is activated by noxious temperatures and we did not observe the mice actively exploring regions of the assay at or above noxious temperature thresholds in this study.

However, while TrpV1 knockouts are mostly indistinguishable from their wild type counterparts in innocuous thermal sensitivity, they fail to develop thermal allodynia and hyperalgesia during inflammation,<sup>54,55</sup> implying an increased role for TrpV1 activity in inflammation. Indeed, TrpV1 has a lower thermal threshold in cases of inflammatory pain and this effect is likely mediated by phosphorylation-dependent upregulation of channel function through inflammatory mediators.<sup>56–58</sup> TrpV1 has multiple potential targets sites for phosphorylation by protein kinases. There is a large body of evidence to support the role of protein kinase C (PKC) and protein kinase A (PKA) signalling pathways in the sensitization of TrpV1.<sup>56–58</sup> PKC, activated via bradykinin, phosphorylates TrpV1 and potentiates heat-evoked responses by lowering the threshold temperature for channel activation.<sup>57,59–61</sup> TrpV1 is also known to be sensitized through the prostaglandin-mediated activation of PKA.<sup>62,63</sup> Capsaicin has been shown to result in peripheral neurogenic inflammation.<sup>64</sup> This is often

characterized by the sustained release of an “inflammatory soup” which most notably consists of the peptides Substance-P and Calcitonin gene-related peptide (CGRP), that are released from peripheral terminals of primary afferents that trigger the release of additional mediators from non-neuronal cells, such as bradykinin, prostaglandins and neurotrophins (NGF).<sup>65</sup> Overall, the sensitization of TrpV1 renders TrpV1<sup>+</sup> afferents more excitable and lowers their thermal threshold of activation. This peripheral inflammatory process likely contributed to the change in thermal preference of mice after intraplantar injection of capsaicin. In support of this, we observed that gabapentin reduced thermal preference of mice injected with capsaicin. Gabapentin exerts part of its analgesic properties through its ability to reduce the presence of inflammatory mediators.<sup>66</sup> As a result, this mechanism may explain how gabapentin was able to reverse the effect of capsaicin-induced warm temperature aversion.

We unexpectedly observed that acute peri-threshold optogenetic activation of TrpV1<sup>+</sup> afferent terminals in the spinal cord did not alter thermal preference. This finding suggests that the central activation of TrpV1<sup>+</sup> afferents itself is insufficient to induce changes in thermal preference, which is likely driven by the multiple factors that contribute to the difference between capsaicin-induced neuronal activation and optogenetic activation of central TrpV1<sup>+</sup> afferent terminals. The breeding strategy used to obtain TrpV1-ChR2 mice generates a fate map of TrpV1 expression which is developmentally regulated. TrpV1 is more broadly expressed during embryogenesis and 2-weeks postnatally than in adults. In fact, only 64% of the labelled neurons may respond to capsaicin in the adult transgenic mouse. This suggests that we are activating a broader class of primary afferents in our optogenetic model than the capsaicin one,<sup>31</sup> the effects of which may not be additive. Indeed, selective primary afferent innervation of excitatory and inhibitory interneurons in the spinal dorsal horn allow for varied integration of incoming signals from the periphery.<sup>67</sup> Additionally, artificial single channel driven neuronal activation fails to recapitulate physiological neuronal firing and the change in thermal preference likely requires a host of other changes beyond an increase in the excitability of TrpV1<sup>+</sup> afferents.

The administration of intraplantar capsaicin also causes mechanical hyperalgesia arising from central sensitization.<sup>68</sup> It is possible that central sensitization further contributed to the change in thermal preference observed after capsaicin injection. However, we did not observe a change in thermal preference towards lower temperatures after induction of sensitization by supra-threshold activation of central TrpV1-ChR2 terminals, further supporting the argument that changes in thermal preference caused by intraplantar capsaicin injection

arises from peripheral mechanisms. Alternatively, it is possible that the biophysical differences between TrpV1 and ChR2 channels underlie the inconsistencies in behavioral responses to capsaicin and optogenetic afferent activation: TrpV1 is a non-selective, large pore cation channel with a notable calcium permeability,<sup>69</sup> while ChR2 is a lower conductance cation channel with lower calcium permeability.<sup>70</sup> This raises the possibility that the lack of calcium influx in the optogenetic stimulation paradigm is a factor in the lack of behavioral changes. However, the induction of mechanical sensitization we observed in response to central TrpV1-ChR2 activation implies that our optogenetic protocol is capable of recapitulating the central sensitization associated with intraplantar capsaicin injection.

Our present findings suggest that peripheral inflammation induced by capsaicin may be a crucial process by which thermal sensory changes arise in some pain states. Although not quantified, we also noted a lack of visual signs of inflammation such as redness and edema in the hind paws of the stimulated TrpV1-ChR2 implanted animals, as is typically seen in response to capsaicin. Notably, previously studies optogenetically activating hindleg nociceptors have also failed to produce neurogenic inflammation.<sup>33,39</sup> Specifically, channelrhodopsin-mediated activation of  $\text{Na}_v1.8^{+39}$  and  $\text{TrpV1}^{+33}$  primary afferents has been shown to not produce neurogenic inflammation. We speculate that the likely failure to produce peripheral neurogenic inflammation in this study may further arise from the fact that we were activating central projections of the primary afferent rather than peripheral terminals. Future studies investigating changes in thermal preference in other pain models, including inflammatory models, such as intraplantar injection of CFA and neuropathic models, such as spared nerve injury (SNI), will further reveal whether differing mechanisms of pathological pain have differing consequences on thermal preference.

Usage of automation in pain research is steadily increasing. Facial grimace scales for mice and rats have now been paired with deep neural networks and specialized software, respectively, for recognizing subtle facial expressions that reflect spontaneous pain with accuracy comparable to a trained human evaluator.<sup>71,72</sup> Here we assessed thermal preference using DeepLabCut, an open-source application that trains deep neural networks to track user-identified objects of interest in video recordings without the need of physical markers on the subjects themselves.<sup>42,43</sup> We showed that DeepLabCut could track mice comparably to EthoVision, and that there was high fidelity and consistency in tracking our desired points upon visual inspection on a frame-by-frame basis. However, as the program is limited to only tracking coordinates of individual points, more intricate software or algorithms

must be developed to characterize complex subject behaviors or when working with multiple points, such as hind paw licking after plantar injection of formalin.<sup>73</sup>

A major aim of this study was to produce a low-cost and simple apparatus for assessing thermal preference in mice. The materials used to create the arena, namely the aluminum plate, wires, computer power supply, Plexiglas, heat sinks, cooling fans, and video camera, are readily available and sourced. Furthermore, assembly of the arena and data analysis requires minimal engineering, electronics, or programming expertise. In comparison with commercially available systems, our assay setup resembles Bioseb's Thermal Gradient Test (Bioseb, Chaville, France), whose temperature gradient from 5 to 55°C is created using two temperature modulators acting on opposite ends of a rectangular aluminum-based corridor. Bioseb uses specialized software to analyze video recordings of their trials by separating the aluminum corridor into distinct temperature zones, similar to our video analysis approach. Other academic assays used photobeam or infrared sensors along equally-spaced intervals along the arena for mouse detection as opposed to a camera.<sup>50,53,74</sup> Consequently, estimations of mice positions were limited to discrete locations rather than along a continuous spectrum of positions across the arena. This drawback is shared by 2-plate temperature preference and hot plate tests, in that discrete temperatures may not accurately reflect a mouse's preferred temperature if it falls either in between or outside those chosen temperatures. The temperature range of gradient-based thermal choice assays range from 0.8 to 55.0°C and generally report mice prefer temperatures between 28.6 to 35.0°C,<sup>50,53,74-79</sup> which directly aligns with the boundaries of temperature preferences reported here.

Our assay had a temperature range from approximately 10°C to 50°C so as to allow for possible exposure of the mice to noxious temperatures. As expected, mice did not explore zones in the assay that had aversively high or low temperatures but stayed within a preferred range of temperatures consistent for mice. Depending on the needs of the experimenter, one possible refinement of our assay would be to reduce the range of temperatures along the length of the assay, using either less powerful Peltier devices or by incorporating potentiometers to control the power supplied to the Peltier devices and to modulate the temperature at the ends of the arena. This would reduce the gradient of the temperature change and potentially encourage both increased mouse exploration of the arena within the innocuous temperature range and increased precision of temperature preference estimates.

Notably, different strains, sexes, ages, and housing conditions of mice can affect thermal preference.<sup>51,80,81</sup> For example, older (>11 months) CD-1s prefer warmer

temperatures, whereas older C57BL/6N mice do not.<sup>51,52</sup> Singly housed older CD-1s also prefer warmer conditions than group housed ones, while younger CD-1s did not differ in preference when housed individually or in groups.<sup>80,81</sup> Furthermore, female mice also tend to prefer warmer temperatures than males, likely attributed to differing metabolic needs, body composition, and hormonal physiology.<sup>51,52</sup> Our assay would allow further research of such physiological variables in temperature preference in addition to the pathological variables examined here. Given that strain differences in thermosensory and thermoregulatory processes<sup>52,82</sup> have been reported, we acknowledge that mouse strain may be a confounding factor for the difference in phenotypic response observed in response to capsaicin injections in CD-1 mice and optogenetic activation of TrpV1<sup>+</sup> neurons in TrpV1-ChR2 mice bred on a C57BL/6N background.

Overall, we report the development and validation of an easily sourced assay for the automated assessment of thermal preference in mice. Using this assay, we confirmed changes in thermal preference induced by peripheral capsaicin injection, and further contrasted these findings against the lack of a change in thermal preference induced by optogenetic stimulation of TrpV1<sup>+</sup> afferents at the level of the spinal cord. These findings support the use of this assay to investigate central and peripheral mechanisms governing thermal preference in freely behaving animals.

### Authors' Contributions

Pharmacological experiments and DeepLabCut animal tracking were performed by JL, optogenetic experiments and associated animal tracking were performed by MZ. JL and MZ analyzed data, and all authors planned the experiments, wrote, and edited the final manuscript.

### Declaration of Conflicting Interests

The authors declared no potential conflicts of interest with respect to the research, authorship, and/or publication of this article.

### Funding

The authors disclosed receipt of the following financial support for the research, authorship, and/or publication of this article: This research was supported by funding from the Natural Sciences and Engineering Research Council of Canada (RGPIN-2016-05538 to RPB), the Canadian Institutes of Health Research (FRN 162179; RPB), a Canada Research Chair in Sensory Plasticity and Reconsolidation (RPB), the Canadian Pain Society (RPB), and the University of Toronto Centre for the Study of Pain (MZ, RPB).

### ORCID iDs

Jerry Li  <https://orcid.org/0000-0002-5178-2706>

Robert P Bonin  <https://orcid.org/0000-0002-3287-6803>

### References

- Courtney CA, Fernandez-de-Las-Penas C, Bond S. Mechanisms of chronic pain – key considerations for appropriate physical therapy management. *J Man Manip Ther* 2017; 25: 118–127.
- Mills SEE, Nicolson KP, Smith BH. Chronic pain: a review of its epidemiology and associated factors in population-based studies. *Br J Anaesth* 2019; 123: e273–e283.
- Duenas M, Ojeda B, Salazar A, Mico JA, Failde I. A review of chronic pain impact on patients, their social environment and the health care system. *J Pain Res* 2016; 9: 457–467.
- Basbaum AI, Bautista DM, Scherrer G, Julius D. Cellular and molecular mechanisms of pain. *Cell* 2009; 139: 267–284.
- Kuner R. Central mechanisms of pathological pain. *Nat Med* 2010; 16: 1258–1266.
- Wong F, Rodrigues A, Schmidt S, Vierck CJ Jr, Mauderli AP. Extreme thermal sensitivity and pain-induced sensitization in a fibromyalgia patient. *Pain Res Treat* 2010; 2010: 912513.
- Ten Brink AF, Goebel A, Berwick R, McCabe CS, Bultitude JH. Sensitivity to ambient temperature increases in fibromyalgia and CRPS. *Pain Med* 2020; 21: 3726–3729.
- Jensen TS, Finnerup NB. Allodynia and hyperalgesia in neuropathic pain: clinical manifestations and mechanisms. *Lancet Neurol* 2014; 13: 924–935.
- Mogil JS, Davis KD, Derbyshire SW. The necessity of animal models in pain research. *Pain* 2010; 151: 12–17.
- Mogil JS. Animal models of pain: progress and challenges. *Nat Rev Neurosci* 2009; 10: 283–294.
- Deuis JR, Dvorakova LS, Vetter I. Methods used to evaluate pain behaviors in rodents. *Front Mol Neurosci* 2017; 10: 284.
- O'Neill J, Brock C, Olesen AE, Andresen T, Nilsson M, Dickenson AH. Unravelling the mystery of capsaicin: a tool to understand and treat pain. *Pharmacol Rev* 2012; 64: 939–971.
- Burma NE, Leduc-Pessah H, Fan CY, Trang T. Animal models of chronic pain: advances and challenges for clinical translation. *J Neurosci Res* 2017; 95: 1242–1256.
- Yeziarski RP, Hansson P. Inflammatory and neuropathic pain from bench to bedside: what went wrong? *J Pain* 2018; 19: 571–588.
- Baliki M, Calvo O, Chialvo DR, Apkarian AV. Spared nerve injury rats exhibit thermal hyperalgesia on an automated operant dynamic thermal escape task. *Mol Pain* 2005; 1: 18.
- Cho C, Michailidis V, Lecker I, Collymore C, Hanwell D, Loka M, Danesh M, Pham C, Urban P, Bonin RP, Martin LJ. Evaluating analgesic efficacy and administration route following craniotomy in mice using the grimace scale. *Sci Rep* 2019; 9: 359.
- Matsumiya LC, Sorge RE, Sotocinal SG, Tabaka JM, Wieskopf JS, Zaloum A, King OD, Mogil JS. Using the Mouse Grimace Scale to reevaluate the efficacy of

- postoperative analgesics in laboratory mice. *J Am Assoc Lab Anim Sci* 2012; 51: 42–49.
18. Tappe-Theodor A, Kuner R. Studying ongoing and spontaneous pain in rodents—challenges and opportunities. *Eur J Neurosci* 2014; 39: 1881–1890.
  19. Tappe-Theodor A, King T, Morgan MM. Pros and cons of clinically relevant methods to assess pain in rodents. *Neurosci Biobehav Rev* 2019; 100: 335–343.
  20. Immke DC, Gavva NR. The TRPV1 receptor and nociception. *Semin Cell Dev Biol* 2006; 17: 582–591.
  21. Yang F, Zheng J. Understand spiciness: mechanism of TRPV1 channel activation by capsaicin. *Protein Cell* 2017; 8: 169–177.
  22. Zygmunt PM, Petersson J, Andersson DA, Chuang H, Sorgard M, Di Marzo V, Julius D, Hogestatt ED. Vanilloid receptors on sensory nerves mediate the vasodilator action of anandamide. *Nature* 1999; 400: 452–457.
  23. Jordt SE, Tominaga M, Julius D. Acid potentiation of the capsaicin receptor determined by a key extracellular site. *Proc Natl Acad Sci U S A* 2000; 97: 8134–8139.
  24. Gilchrist HD, Allard BL, Simone DA. Enhanced withdrawal responses to heat and mechanical stimuli following intraplantar injection of capsaicin in rats. *Pain* 1996; 67: 179–188.
  25. Soliman AC, Yu JS, Coderre TJ. mGlu and NMDA receptor contributions to capsaicin-induced thermal and mechanical hypersensitivity. *Neuropharmacology* 2005; 48: 325–332.
  26. Sandkuhler J. Models and mechanisms of hyperalgesia and allodynia. *Physiol Rev* 2009; 89: 707–758.
  27. Yalcin I, Charlet A, Freund-Mercier MJ, Barrot M, Poisbeau P. Differentiating thermal allodynia and hyperalgesia using dynamic hot and cold plate in rodents. *J Pain* 2009; 10: 767–773.
  28. Decosterd I, Woolf CJ. Spared nerve injury: an animal model of persistent peripheral neuropathic pain. *Pain* 2000; 87: 149–158.
  29. Shields SD, Eckert WA, 3rd, Basbaum AI. Spared nerve injury model of neuropathic pain in the mouse: a behavioral and anatomic analysis. *J Pain* 2003; 4: 465–470.
  30. Allchorne AJ, Broom DC, Woolf CJ. Detection of cold pain, cold allodynia and cold hyperalgesia in freely behaving rats. *Mol Pain* 2005; 1: 36.
  31. Cavanaugh DJ, Chesler AT, Braz JM, Shah NM, Julius D, Basbaum AI. Restriction of transient receptor potential vanilloid-1 to the peptidergic subset of primary afferent neurons follows its developmental downregulation in nonpeptidergic neurons. *J Neurosci* 2011; 31: 10119–10127.
  32. Beaudry H, Daou I, Ase AR, Ribeiro-da-Silva A, Seguela P. Distinct behavioral responses evoked by selective optogenetic stimulation of the major TRPV1+ and MrgD+ subsets of C-fibers. *Pain* 2017; 158: 2329–2339.
  33. Stemkowski P, Garcia-Caballero A, De Maria Gadotti V, M'Dahoma S, Huang S, Gertrud Black SA, Chen L, Souza IA, Zhang Z, Zamponi GW. TRPV1 nociceptor activity initiates USP5/T-type channel-mediated plasticity. *Cell Rep* 2017; 18: 2289–2290.
  34. Moehring F, Cowie AM, Menzel AD, Weyer AD, Grzybowski M, Arzua T, Geurts AM, Palygin O, Stucky CL. Keratinocytes mediate innocuous and noxious touch via ATP-P2X4 signaling. *Elife* 2018; 7: e31684.
  35. Albisetti GW, Pagani M, Platonova E, Hosli L, Johannssen HC, Fritschy JM, Wildner H, Zeilhofer HU. Dorsal horn gastrin-releasing peptide expressing neurons transmit spinal itch but not pain signals. *J Neurosci* 2019; 39: 2238–2250.
  36. Bonin RP, Wang F, Desrochers-Couture M, Ga Secka A, Boulanger M-E, Côté DC, De Koninck Y. Epidural optogenetics for controlled analgesia. *Mol Pain* 2016; 12: 1–11.
  37. Christensen AJ, Iyer SM, Francois A, Vyas S, Ramakrishnan C, Vesuna S, Deisseroth K, Scherrer G, Delp SL. In vivo interrogation of spinal mechanosensory circuits. *Cell Rep* 2016; 17: 1699–1710.
  38. Zhang H, Lecker I, Collymore C, Dokova A, Pham MC, Rosen SF, Crawhall-Duk H, Zain M, Valencia M, Filippini HF, Li J, D'Souza AJ, Cho C, Michailidis V, Whissell PD, Patel I, Steenland HW, Virginia Lee WJ, Moayed M, Sterley TL, Bains JS, Stratton JA, Matyas JR, Biernaskie J, Dubins D, Vukobradovic I, Bezginov A, Flenniken AM, Martin LJ, Mogil JS, Bonin RP. Cage-lid hanging behavior as a translationally relevant measure of pain in mice. *Pain*. Epub ahead of print 25 November 2020. DOI: 10.1097/j.pain.0000000000002127.
  39. Daou I, Tuttle AH, Longo G, Wieskopf JS, Bonin RP, Ase AR, Wood JN, De Koninck Y, Ribeiro-da-Silva A, Mogil JS, Seguela P. Remote optogenetic activation and sensitization of pain pathways in freely moving mice. *J Neurosci* 2013; 33: 18631–18640.
  40. Bonin RP, Bories C, De Koninck Y. A simplified up-down method (SUDO) for measuring mechanical nociception in rodents using von Frey filaments. *Mol Pain* 2014; 10: 26.
  41. Zain M, Bonin RP. Alterations in evoked and spontaneous activity of dorsal horn wide dynamic range neurons in pathological pain: a systematic review and analysis. *Pain* 2019; 160: 2199–2209.
  42. Nath T, Mathis A, Chen AC, Patel A, Bethge M, Mathis MW. Using DeepLabCut for 3D markerless pose estimation across species and behaviors. *Nat Protoc* 2019; 14: 2152–2176.
  43. Mathis A, Mamidanna P, Cury KM, Abe T, Murthy VN, Mathis MW, Bethge M. DeepLabCut: markerless pose estimation of user-defined body parts with deep learning. *Nat Neurosci* 2018; 21: 1281–1289.
  44. Noldus LP, Spink AJ, Tegelenbosch RA. EthoVision: a versatile video tracking system for automation of behavioral experiments. *Behav Res Methods Instrum Comput* 2001; 33: 398–414.
  45. Pham J, Cabrera SM, Sanchis-Segura C, Wood MA. Automated scoring of fear-related behavior using EthoVision software. *J Neurosci Methods* 2009; 178: 323–326.
  46. Spink AJ, Tegelenbosch RA, Buma MO, Noldus LP. The EthoVision video tracking system – a tool for behavioral phenotyping of transgenic mice. *Physiol Behav* 2001; 73: 731–744.

47. Negus SS. Core outcome measures in preclinical assessment of candidate analgesics. *Pharmacol Rev* 2019; 71: 225–266.
48. Kuner R, Flor H. Structural plasticity and reorganisation in chronic pain. *Nat Rev Neurosci* 2016; 18: 20–30.
49. Wang TA, Teo CF, Akerblom M, Chen C, Tynan-La Fontaine M, Greiner VJ, Diaz A, McManus MT, Jan YN, Jan LY. Thermoregulation via temperature-dependent PGD2 production in mouse preoptic area. *Neuron* 2019; 103: 309 e307–322 e307.
50. Lee H, Iida T, Mizuno A, Suzuki M, Caterina MJ. Altered thermal selection behavior in mice lacking transient receptor potential vanilloid 4. *J Neurosci* 2005; 25: 1304–1310.
51. Gaskill BN, Gordon CJ, Pajor EA, Lucas JR, Davis JK, Garner JP. Heat or insulation: behavioral titration of mouse preference for warmth or access to a nest. *PLoS One* 2012; 7: e32799.
52. Gaskill BN, Rohr SA, Pajor EA, Lucas JR, Garner JP. Some like it hot: mouse temperature preferences in laboratory housing. *Appl Anim Behav Sci* 2009; 116: 279–285.
53. Shimizu I, Iida T, Guan Y, Zhao C, Raja SN, Jarvis MF, Cockayne DA, Caterina MJ. Enhanced thermal avoidance in mice lacking the ATP receptor P2X3. *Pain* 2005; 116: 96–108.
54. Caterina MJ, Leffler A, Malmberg AB, Martin WJ, Trafton J, Petersen-Zeitz KR, Koltzenburg M, Basbaum AI, Julius D. Impaired nociception and pain sensation in mice lacking the capsaicin receptor. *Science* 2000; 288: 306–313.
55. Davis JB, Gray J, Gunthorpe MJ, Hatcher JP, Davey PT, Overend P, Harries MH, Latcham J, Clapham C, Atkinson K, Hughes SA, Rance K, Grau E, Harper AJ, Pugh PL, Rogers DC, Bingham S, Randall A, Sheardown SA. Vanilloid receptor-1 is essential for inflammatory thermal hyperalgesia. *Nature* 2000; 405: 183–187.
56. Li L, Hasan R, Zhang X. The basal thermal sensitivity of the TRPV1 ion channel is determined by PKC $\beta$ II. *J Neurosci* 2014; 34: 8246–8258.
57. Wang S, Joseph J, Ro JY, Chung MK. Modality-specific mechanisms of protein kinase C-induced hypersensitivity of TRPV1: S800 is a polymodal sensitization site. *Pain* 2015; 156: 931–941.
58. Ilie MA, Caruntu C, Tampa M, Georgescu SR, Matei C, Negrei C, Ion RM, Constantin C, Neagu M, Boda D. Capsaicin: physicochemical properties, cutaneous reactions and potential applications in painful and inflammatory conditions. *Exp Ther Med* 2019; 18: 916–925.
59. Numazaki M, Tominaga T, Toyooka H, Tominaga M. Direct phosphorylation of capsaicin receptor VR1 by protein kinase C $\epsilon$  and identification of two target serine residues. *J Biol Chem* 2002; 277: 13375–13378.
60. Zhang X, Li L, McNaughton PA. Proinflammatory mediators modulate the heat-activated ion channel TRPV1 via the scaffolding protein AKAP79/150. *Neuron* 2008; 59: 450–461.
61. Sugiura T, Tominaga M, Katsuya H, Mizumura K. Bradykinin lowers the threshold temperature for heat activation of vanilloid receptor 1. *J Neurophysiol* 2002; 88: 544–548.
62. Mohapatra DP, Nau C. Desensitization of capsaicin-activated currents in the vanilloid receptor TRPV1 is decreased by the cyclic AMP-dependent protein kinase pathway. *J Biol Chem* 2003; 278: 50080–50090.
63. Moriyama T, Higashi T, Togashi K, Iida T, Segi E, Sugimoto Y, Tominaga T, Narumiya S, Tominaga M. Sensitization of TRPV1 by EP1 and IP reveals peripheral nociceptive mechanism of prostaglandins. *Mol Pain* 2005; 1: 3.
64. Holst H, Arendt-Nielsen L, Mosbech H, Serup J, Elberling J. Capsaicin-induced neurogenic inflammation in the skin in patients with symptoms induced by odorous chemicals. *Skin Res Technol* 2011; 17: 82–90.
65. Julius D, Basbaum AI. Molecular mechanisms of nociception. *Nature* 2001; 413: 203–210.
66. Anfuso CD, Olivieri M, Fidilio A, Lupo G, Rusciano D, Pezzino S, Gagliano C, Drago F, Bucolo C. Gabapentin attenuates ocular inflammation: in vitro and in vivo studies. *Front Pharmacol* 2017; 8: 173.
67. Harding EK, Fung SW, Bonin RP. Insights into spinal dorsal horn circuit function and dysfunction using optical approaches. *Front Neural Circuits* 2020; 14: 31.
68. Bonin RP, De Koninck Y. A spinal analog of memory reconsolidation enables reversal of hyperalgesia. *Nat Neurosci* 2014; 17: 1043–1045.
69. Munns CH, Chung MK, Sanchez YE, Amzel LM, Caterina MJ. Role of the outer pore domain in transient receptor potential vanilloid 1 dynamic permeability to large cations. *J Biol Chem* 2015; 290: 5707–5724.
70. Beck S, Yu-Strzelczyk J, Pauls D, Constantin OM, Gee CE, Ehmann N, Kittel RJ, Nagel G, Gao S. Synthetic light-activated ion channels for optogenetic activation and inhibition. *Front Neurosci* 2018; 12: 643.
71. Tuttle AH, Molinaro MJ, Jethwa JF, Sotocinal SG, Prieto JC, Styner MA, Mogil JS, Zylka MJ. A deep neural network to assess spontaneous pain from mouse facial expressions. *Mol Pain* 2018; 14: 1744806918763658.
72. Sotocinal SG, Sorge RE, Zaloum A, Tuttle AH, Martin LJ, Wieskopf JS, Mapplebeck JC, Wei P, Zhan S, Zhang S, McDougall JJ, King OD, Mogil JS. The Rat Grimace Scale: a partially automated method for quantifying pain in the laboratory rat via facial expressions. *Mol Pain* 2011; 7: 55.
73. Recla JM, Bubier JA, Gatti DM, Ryan JL, Long KH, Robledo RF, Glidden NC, Hou G, Churchill GA, Maser RS, Zhang ZW, Young EE, Chesler EJ, Bult CJ. Genetic mapping in diversity outbred mice identifies a Trpa1 variant influencing late-phase formalin response. *Pain* 2019; 160: 1740–1753.
74. Gordon CJ, Bailey EB, Kozel WM, Ward GH. A device for monitoring position of unrestrained animals in a temperature gradient. *Physiol Behav* 1983; 31: 265–268.
75. Kaikaew K, Steenbergen J, Themmen APN, Visser JA, Grefhorst A. Sex difference in thermal preference of adult mice does not depend on presence of the gonads. *Biol Sex Differ* 2017; 8: 24.
76. Gordon CJ, Kimm-Brinson KL, Padnos B, Ramsdell JS. Acute and delayed thermoregulatory response of mice exposed to brevetoxin. *Toxicol* 2001; 39: 1367–1374.



77. Huang T, Lin SH, Malewicz NM, Zhang Y, Zhang Y, Goulding M, LaMotte RH, Ma Q. Identifying the pathways required for coping behaviors associated with sustained pain. *Nature* 2019; 565: 86–90.
78. Huang SM, Li X, Yu Y, Wang J, Caterina MJ. TRPV3 and TRPV4 ion channels are not major contributors to mouse heat sensation. *Mol Pain* 2011; 7: 37.
79. Marics I, Malapert P, Reynders A, Gaillard S, Moqrich A. Acute heat-evoked temperature sensation is impaired but not abolished in mice lacking TRPV1 and TRPV3 channels. *PLoS One* 2014; 9: e99828.
80. Gordon CJ, Becker P, Ali JS. Behavioral thermoregulatory responses of single- and group-housed mice. *Physiol Behav* 1998; 65: 255–262.
81. Jirkof P, Bratcher N, Medina L, Strasburg D, Ebert P, Gaskill BN. The effect of group size, age and handling frequency on inter-male aggression in CD 1 mice. *Sci Rep* 2020; 10: 2253.
82. Gaskill BN, Gordon CJ, Pajor EA, Lucas JR, Davis JK, Garner JP. Impact of nesting material on mouse body temperature and physiology. *Physiol Behav* 2013; 110–111: 87–95.